ACS APPLIED MATERIALS & INTERFACES

Letter

www.acsami.org

Tunable Surface and Matrix Chemistries in Optically Printed (0−3) Piezoelectric Nanocomposites

Kanguk Kim,[†,‡] James L. Middlebrook,[†,§] Jeffrey E. Chen,[§] Wei Zhu,[§] Shaochen Chen,[‡,§] and Donald J. Sirbuly*[,‡,§]

[‡]Materials Science and Engineering and [§]Department of NanoEngineering, University of California, San Diego, La Jolla, California 92093, United States

Supporting Information

ABSTRACT: In this work, the impacts of varying surface modification, matrix parameters, and fabrication conditions on the performance of optically printed (0−3) piezoelectric polymer nanocomposites are examined. For example, we find that a 75% reduction in nanoparticle edge-length boosted the piezoelectric coefficient (d_{33}) by over 100%. By optimizing the composition and fabrication conditions, 10% by mass loading barium titanate nanocomposites are able to yield d_{33} values of ∼80 pC/N compared to <5 pC/N when parameters are not optimized. With a more complete understanding of how to enhance the performance of (0−3) piezoelectric polymer nanocomposites, these materials should find use in a wide range of applications.

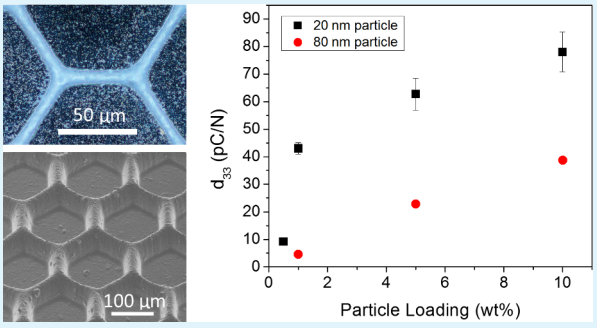

KEYWORDS: *piezoelectric, nanocomposite, 3D printing, nanoparticle, polymerization, polymer*

Piezoelectric materials and their ability to couple mechanical and electrical energy forms have played important roles in applications such as nanogenerators,[1,2] sensors,[3,4] and ultrasonic transducers.[5,6] Conventional inorganic piezoelectric materials such as lead zirconate titanate (PZT) are most commonly used in the form of large, bulk electroceramics due to their high piezoelectric coefficients.[7] However, this bulk electroceramic implementation restricts these materials' applications due to inherent limitations such as poor mechanical flexibility, brittleness,[8−10] and in the case of PZT, the presence of lead which limits biological applications.[11] Piezoelectric polymers, such as polyvinylidene fluoride (PVDF), have been proposed as candidates to help circumvent these issues, but their piezoelectric coefficients are typically an order of magnitude less than that of ceramic-based piezoelectric materials.[12] While both ceramic and polymer piezoelectrics have their advantages and disadvantages, piezoelectric nanocomposites have garnered significant attention as an alternative material that bridges the gap between bulk electroceramics and pure polymer piezoelectrics by providing moderate piezoelectric coefficients while retaining mechanical flexibility and biocompatibility. These nanocomposites typically take the form of one-dimensional piezoelectric ceramics such as nanowires or rods embedded in a polymer matrix, known as a (1−3) composite,[13,14] or nanoparticles suspended in a matrix, a (0−3) composite.[15−19] As the potential for these composite materials grows to fill this void in modern piezoelectrics, it is important to explore the ability to control the ceramic−polymer interface and the effects from changing the properties of the polymer matrix.[20,21]

In previous work, we demonstrated that piezoelectric (0−3) nanoparticle−polymer composite materials could be optically printed in three dimensions (3D) using barium titanate (BT) nanoparticles suspended in a photoliable polymer solution.[22] Through the use of a digital projection printing (DPP) method, we were able to selectively cross-link regions of the solution using ultraviolet (UV) light and a photopolymerizable polymer such as poly(ethylene glycol diacrylate) (PEGDA). As the polymer cross-links under light exposure, the BT nanoparticles are encased in the matrix, allowing feature sizes as a small as 5 μm to be reproducibly fabricated. It was also demonstrated that grafting acrylate containing surface groups, such as 3-(trimethoxysilyl)propyl methacrylate (TMSPM), onto the BT enhanced the stress-transfer efficiency by an order of magnitude.[22] These linkers are a critical component to understanding how to tune the performance of piezoelectric nanocomposites since they significantly increase the inorganic-polymer interfacial interaction. In this work, we examine a wide parameter space, including different linker molecules, changes in the polymer's molecular weight, microstructure size, and nanoparticle size, to obtain a more complete understanding on how to better engineer piezoelectric polymer nanocomposites. Although the BT-PEDGA system is studied here, the findings should be universal for other nanoparticle-photopolymer systems.

Received: September 23, 2016
Accepted: November 28, 2016
Published: November 28, 2016

DOI: 10.1021/acsami.6b12086
ACS Appl. Mater. Interfaces 2016, 8, 33394−33398

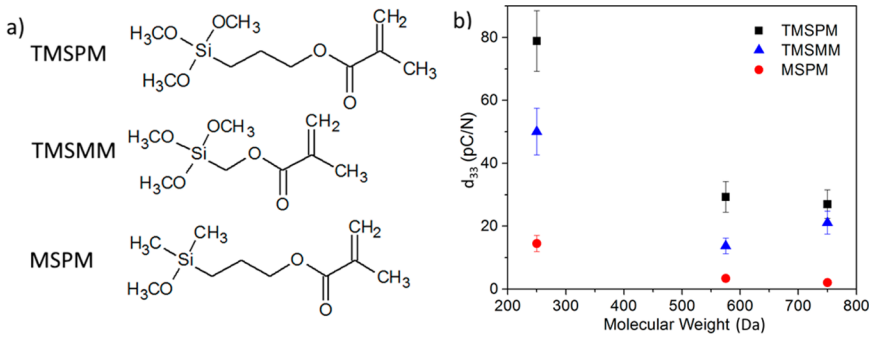

Figure 1. (a) Structures of methacrylate silane molecules used to functionalize the surface of the BT nanoparticles including 3-(trimethoxysilyl)propyl methacrylate (TMSPM), 3-(trimethoxysilyl)methyl methacrylate (TMSMM), and 3-(methoxydimethylsilyl)propyl methacrylate (MSPM). (b) Piezoelectric coefficients (d_{33}) for unstructured PEGDA thin films (125 μm thick) with a 10% mass loading of 80 nm BT nanoparticles. The BT was surface functionalized with TMSPM (square), MSPM (circle), or TMSMM (triangle). The PEGDA molecular weights used were 258, 575, and 750 Da.

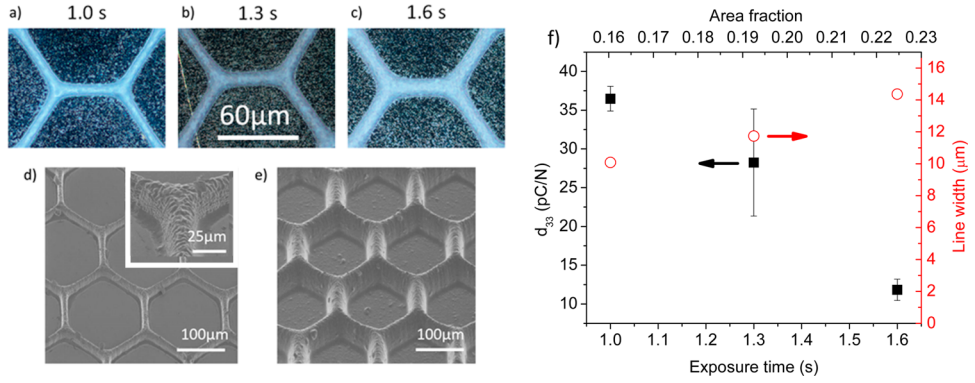

Figure 2. Optical images of honeycomb arrays printed with UV exposure times of (a) 1.0, (b) 1.3, and (c) 1.6 s. Scanning electron micrographs of the patterned structures produced with UV exposure times of (d) 1.0 and (e) 1.6 s. (f) Measured d_{33} coefficients and line widths of the honeycomb arrays as a function of exposure time/area fraction. All samples were prepared with 80 nm BT nanoparticles with a 10% mass loading.

There is a strong relationship between the piezoelectric output of optically printed composite materials and the piezoelectric nanoparticles' ability to mechanically couple to the matrix. Larger electrical outputs are the result of a stronger interaction between the active piezoelectric crystal and the stresses acting on the polymer. As previously shown, the presence of the TMSPM linker group on the BT nanoparticle surface is far more effective in producing a piezoelectric output compared to unmodified nanoparticles entrapped in a pure polymer matrix or even a nanocomposite doped with carbon nanotubes to enhance the mechanical properties. In order to better understand the role of these chemical linker molecules in transferring mechanical stress, TMSPM modified particle composites were compared against composites containing particles functionalized with linker variants, 3-(trimethoxysilyl)-methyl methacrylate (TMSMM) and 3-(methoxydimethylsilyl)propyl methacrylate (MSPM) (Figure 1a). These variants were chosen to closely mimic the chemical nature of TMSPM, but alter the number of silyl ether (Si−O-R) groups, which act as binding sites to the nanoparticles. or shorten the central carbon chain, which influences the degrees of freedom between the BT and the polymer matrix. In addition, the impact of polymer stiffness was examined by changing its molecular weight. Polymers such as PEG have been shown to become stiffer as the molecular weight is decreased.[23]

To test the piezoelectric properties of the nanocomposites with various linker molecules and polymer molecular weights, linker-modified BT piezoelectric nanoparticles were incorporated into PEGDA composite thin film devices. The composites were fabricated with each of the different linkers (TMSPM, MSPM, TMSMM) as well as with varied PEGDA molecular weights. The materials' piezoelectric charge coefficient (d_{33}, which measures the induced polarization along the 3 direction parallel to the polarized axis, whereas the stress is applied along the same axis) were then measured through an in-house built quasi-static d_{33} meter (data summarized in Figure 1b). A schematic for the force sensor circuit used to measure forces simultaneously with the electrical outputs can be found in Figure S5. Both MSPM and TMSMM functionalized composites exhibit lower piezoelectric coefficients compared to those modified with TMSPM despite the subtle differences in the molecular structures of the linkers. The role of the linker molecules is to form strong links between the matrix and the piezoelectric nanoparticle, and the small differences between the linker molecules can lead to variations in the stress-transfer efficiency. In the case of TMSMM, the shorter central carbon chain places the acrylate group in closer proximity to the silyl binding sites where the nanoparticle is linked. This pulls electron density away from the Si−O−BT bonds resulting in a lower bond strength; translating to a lessened ability to efficiently transfer mechanical stress from the polymer matrix to the piezoelectric ceramic and a lowered piezoelectric coefficient. For MSPM, the reduction in the number of silyl ether groups produces a weaker linkage between the BT nanoparticle and polymer matrix thus also lowering the

DOI: 10.1021/acsami.6b12086
ACS Appl. Mater. Interfaces 2016, 8, 33394−33398

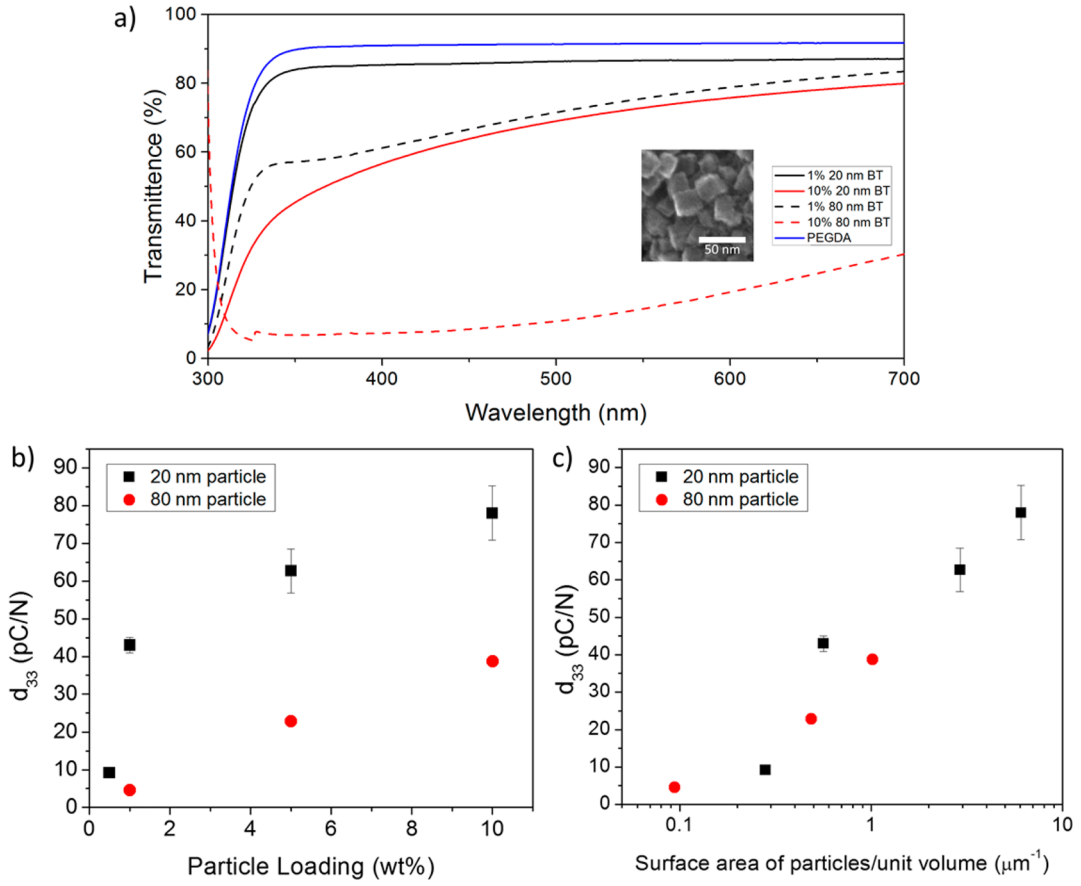

Figure 3. (a) Optical extinction spectra for 10 μm thick PEGDA composite films with 1 or 10% particle loading by weight of 20 or 80 nm BT nanoparticles with inset of scanning transmission electron microscope image of as-made 20 nm BT nanoparticles. (b) Piezoelectric coefficients (d_{33}) as a function of particle loading percentage for 20 nm barium titanate nanoparticles (square) and 80 nm barium titanate nanoparticles (circle) in 25 μm PEGDA film devices. (c) Piezoelectric coefficients (same samples as b) plotted as a logarithmic function of particle surface area per unit volume.

mechanical-to-electrical energy conversion efficiency. Surprisingly, there is nearly a 3× enhancement observed in the piezoelectric coefficient for the lowest polymer molecular weight. Atomic force microscopy measurements show that the stiffness of the PEGDA increases from 252 MPa for the 750 Da polymer to 3.74 GPa for the 258 Da polymer. Increasing the polymer stiffness reduces the mismatch in hardness between the nanoparticle and polymer. This translates to a matrix that can transfer more of the applied stress to the piezoelectric nanoparticles by reducing the number of unproductive deformation modes (e.g., polymer expansion orthogonal to the applied stress) found in softer matrices.

Although there is a strong piezoelectric dependence on chemical factors, other parameters such as the size and shape of the 3D printed microstructures can also influence the piezoelectric response. For example, the area fraction of the piezoelectric polymer in the printed materials can be controlled by tuning the light exposure (Figure 2). Using the same optical mask such as a honeycomb pattern, multiple structure variations can be constructed by increasing the UV exposure time. For example, the honeycomb line width can be increased by ~40% by lengthening the UV exposure from 1.0 to 1.6 s. This slight change in the area fraction results in a ~ 67% decrease in the d_{33} value. All of these hexagonal arrays were printed using the 256 Da PEGDA, but similar trends were observed for the other nanocomposites. The drop in the mechanical-to-electrical energy conversion efficiency for the larger area fractions is likely caused by an increase in the effective elastic modulus. Although the exact same composite is being used, the microstructure of the additionally exposed patterns is less capable of transferring stress to the entrapped nanoparticles and therefore shows a lower charge coefficient compared to the lower area fraction structures. This could be due to the increase in active area or an increase in the cross-link density in the region. It is important to note that the amount of charge generated by the printed films under a load is directly related to the strain rate and the rate of charge-loss in the composite. Therefore, a higher strain rate will produce a larger amount of charge on the surface of the piezoelectric given that the samples being compared have the same rate of charge loss. This effect is observed in the printed microstructures by reducing the amount of active material in the array.

One of the major challenges for optically printing structures with small feature sizes, yet a large volume (e.g., thicker), is creating prepolymerized composite solutions that have high optical transparencies. The PEGDA, or other photocurable polymers, have fairly low absorption coefficients; however, the BT nanoparticles can significantly attenuate light propagation through the composite due to large optical scattering and/or absorption. These light-matter interactions can distort the optical image and cause aberrations in the printed structures past depths of ~300 μm when an above exposure method (i.e., light has to penetrate previously printed regions to access the new layer being printed) is used. Although other exposure

DOI: 10.1021/acsami.6b12086
ACS Appl. Mater. Interfaces 2016, 8, 33394−33398

methods such as extruding the structure away from the light source can be used to circumvent this issue, the light-matter interactions can be mitigated through the composition of the composite. Lower mass loadings (<10%) are required to achieve adequate optical transparencies with the 80 nm nanoparticles, which limits the amount of active piezoelectric particles that can be used and thus the piezoelectric properties. However, the implementation of smaller BT nanoparticles reduces light-matter interactions to allow higher mass loadings while retaining the optical transparency required for printing. In addition, smaller nanoparticles enhance the interfacial area between the BT and the polymer matrix, which should also contribute to a more efficient stress-transfer efficiency. To investigate the effects from nanoparticle size we compared the optical properties of composites made with 80 and 20 nm edge-lengths (Figure 3a). From the transmission experiments it is clear that there is nearly a 7× decrease in the extinction (at 365 nm) going from a printed film loaded with 10% of the larger nanoparticles to the same mass loading with the smaller nanoparticles. In fact, there is only about a 5% drop in the transmittance when a pure PEGDA film is loaded with 1% of the small nanoparticles compared to a ∼30% drop with the 80 nm nanoparticles. The maximum spatial resolution that can be achieved with the system is ∼1 μm using the pure PEGDA. This requires a transmittance at 365 nm of >65% which is only achievable with the smaller nanoparticles. If high spatial resolution is required with the composites, along with larger BT loadings, photoinitiators with longer wavelength absorptions maxima (>500 nm) can be used.

Testing the piezoelectric performance of the smaller nanoparticle composites showed an immediate trend with the smaller nanoparticles outperforming the larger nanoparticles for every mass loading tested (Figure 3b). All materials were poled under the same conditions (10.2 MV/m at 135 °C for 4 h), had identical thicknesses (25 μm), and similar electrode designs. An enhancement of ∼100% is observed for the 20 nm particle composite loaded at 10%, which implies there are contributions from surface area and the number of grafting sites per unit volume. When the charge coefficient is plotted versus the log of the BT surface area per volume of composite (Figure 3c), there is a clear indication that the matrix-nanoparticle interfacial area is one of the most significant parameters that influences the piezoelectric performance. The materials tested with a 0.5% mass loading of 80 nm nanoparticles did not show any measurable signals, suggesting that a surface area to unit volume ratio of 0.2 μm^{-1} is the threshold for piezoelectric behavior in these composites. Although the piezoelectric coefficients do increase with larger mass loading percentages, it is expected that the logarithmic trend ceases at higher mass loadings due to larger particle−particle interactions which limits the nanoparticle−polymer interactions and lowers the stress-transfer efficiency. In addition, successfully printing films with larger mass loadings is difficult due to the increased optical scattering and absorption which prevents complete photo-cross-linking. Understanding and optimizing these nanointerfacial effects is critical for pushing the performance limits of piezoelectric polymer nanocomposites, and optical printing should play a major role in advancing these materials.

In this work, we have demonstrated that the piezoelectric performance of optically printed (0−3) piezoelectric nanocomposites is strongly dependent on parameters such as surface linker chemistry, matrix mechanical properties, and nanoparticle size. With continued investigation on the strengthening and maximization of the stress-transfer efficiency at the inorganic−organic interface, it should be possible to fabricate composite materials with properties that exceed their ceramic monolith counterparts with less active material. Finally, optical printing with UV-curable polymers has been shown to be an ideal platform to systematically study and tune the piezoelectric properties of nanocomposites and offers one of the only routes to high precision, rapid, and 3D fabrication of piezoelectric polymers.

■ ASSOCIATED CONTENT

Supporting Information

The Supporting Information is available free of charge on the ACS Publications website at DOI: 10.1021/acsami.6b12086.

Materials and methods; BT characterization including microscopy, XRD, FTIR, and thermogravimetric analysis; and piezoelectric testing setup (PDF)

■ AUTHOR INFORMATION

Corresponding Author

*E-mail: dsirbuly@ucsd.edu.

ORCID

Jeffrey E. Chen: 0000-0002-6662-6714

Donald J. Sirbuly: 0000-0003-2931-6570

Author Contributions

†K.K. and J.L.M. contributed equally to the work.

Notes

The authors declare no competing financial interest.

■ ACKNOWLEDGMENTS

This work was supported in part by grants from the National Science Foundation (Grant No. 1547005, 1332681) to S.C.

■ REFERENCES

(1) Wang, X. D.; Song, J. H.; Liu, J.; Wang, Z. L. Direct-Current Nanogenerator Driven by Ultrasonic Waves. *Science* **2007**, *316*, 102−105.

(2) Zhu, G. A.; Yang, R. S.; Wang, S. H.; Wang, Z. L. Flexible High-Output Nanogenerator Based on Lateral ZnO Nanowire Array. *Nano Lett.* **2010**, *10*, 3151−3155.

(3) Tadigadapa, S.; Mateti, K. Piezoelectric Mems Sensors: State-of-the-Art and Perspectives. *Meas. Sci. Technol.* **2009**, *20*, 092001.

(4) Zhou, J.; Gu, Y. D.; Fei, P.; Mai, W. J.; Gao, Y. F.; Yang, R. S.; Bao, G.; Wang, Z. L. Flexible Piezotronic Strain Sensor. *Nano Lett.* **2008**, *8*, 3035−3040.

(5) Zhang, S. J.; Li, F.; Jiang, X. N.; Kim, J.; Luo, J.; Geng, X. C. Advantages and Challenges of Relaxor-$PbTiO_3$ Ferroelectric Crystals for Electroacoustic Transducers - a Review. *Prog. Mater. Sci.* **2015**, *68*, 1−66.

(6) Zhou, Q. F.; Lau, S. T.; Wu, D. W.; Shung, K. Piezoelectric Films for High Frequency Ultrasonic Transducers in Biomedical Applications. *Prog. Mater. Sci.* **2011**, *56*, 139−174.

(7) Haertling, G. H. Ferroelectric Ceramics: History and Technology. *J. Am. Ceram. Soc.* **1999**, *82*, 797−818.

(8) Morelli, A.; Johann, F.; Schammelt, N.; Vrejoiu, I. Ferroelectric Nanostructures Fabricated by Focused-Ion-Beam Milling in Epitaxial $BiFeO_3$ Thin Films. *Nanotechnology* **2011**, *22*, 265303.

(9) Alexe, M.; Harnagea, C.; Hesse, D.; Gosele, U. Patterning and Switching of Nanosize Ferroelectric Memory Cells. *Appl. Phys. Lett.* **1999**, *75*, 1793−1795.

(10) Ganpule, C. S.; Stanishevsky, A.; Aggarwal, S.; Melngailis, J.; Williams, E.; Ramesh, R.; Joshi, V.; Paz de Araujo, C. Scaling of Ferroelectric and Piezoelectric Properties in Pt/$SrBi_2Ta_2O_9$/Pt Thin Films. *Appl. Phys. Lett.* **1999**, *75*, 3874−3876.

DOI: 10.1021/acsami.6b12086
ACS Appl. Mater. Interfaces 2016, 8, 33394−33398

(11) Panda, P. K. Review: Environmental Friendly Lead-Free Piezoelectric Materials. *J. Mater. Sci.* **2009**, *44*, 5049−5062.
(12) Kawai, H. Piezoelectricity of Poly (Vinylidene Fluoride). *Jpn. J. Appl. Phys.* **1969**, *8*, 975−976.
(13) Ramadan, K. S.; Sameoto, D.; Evoy, S. A Review of Piezoelectric Polymers as Functional Materials for Electromechanical Transducers. *Smart Mater. Struct.* **2014**, *23*, 033001.
(14) Park, K. I.; Bae, S. B.; Yang, S. H.; Lee, H. I.; Lee, K.; Lee, S. J. Lead-Free $BaTiO_3$ Nanowires-Based Flexible Nanocomposite Generator. *Nanoscale* **2014**, *6*, 8962−8968.
(15) Levassort, F.; Lethiecq, M.; Desmare, R.; Tran-Huu-Hue, L. P. Effective Electroelastic Moduli of 3−3(0−3) Piezocomposites. *IEEE Trans. Ultrason., Ferroelect., Freq. Contr.* **1999**, *46*, 1028−1034.
(16) Prashanthi, K.; Zhang, H.; Rao, V. R.; Thundat, T. Local Piezoelectric Response of Zno Nanoparticles Embedded in a Photosensitive Polymer. *Phys. Status Solidi RRL* **2012**, *6*, 77−79.
(17) Prashanthi, K.; Miriyala, N.; Gaikwad, R. D.; Moussa, W.; Rao, V. R.; Thundat, T. Vibtrational Energy Harvesting Using Photo-Patternable Piezoelectric Nanocomposite Cantilevers. *Nano Energy* **2013**, *2*, 923−932.
(18) Alluri, N. R.; Saravanakumar, B.; Kim, S. J. Flexible, Hybrid Piezoelectric Film $(BaTi_{(1-X)}Zr_xO_3)$/PVDF Nanogenerator as a Self-Powered Fluid Velocity Sensor. *ACS Appl. Mater. Interfaces* **2015**, *7*, 9831−9840.
(19) Park, K. I.; Lee, M.; Liu, Y.; Moon, S.; Hwang, G. T.; Zhu, G.; Kim, J. E.; Kim, S. O.; Kim, D. K.; Wang, Z. L.; Lee, K. J. Flexible Nanocomposite Generator Made of $BaTiO_3$ Nanoparticles and Graphitic Carbons. *Adv. Mater.* **2012**, *24*, 2999−3004.
(20) Nguyen, V. S.; Rouxel, D.; Vincent, B.; Badie, L.; Dos Santos, F. D.; Lamouroux, E.; Fort, Y. Influence of Cluster Size and Surface Functionalization of Zno Nanoparticles on the Morphology, Thermomechanical and Piezoelectric Properties of P(VDF-TrFE) Nanocomposite Films. *Appl. Surf. Sci.* **2013**, *279*, 204−211.
(21) Dalle Vacche, S.; Oliveira, F.; Leterrier, Y.; Michaud, V.; Damjanovic, D.; Manson, J. A. E. Effect of Silane Coupling Agent on the Morphology, Structure, and Properties of Poly(Vinylidene Fluoride-Trifluoroethylene)/$BaTiO_3$ Composites. *J. Mater. Sci.* **2014**, *49*, 4552−4564.
(22) Kim, K.; Zhu, W.; Qu, X.; Aaronson, C.; McCall, W. R.; Chen, S.; Sirbuly, D. J. 3d Optical Printing of Piezoelectric Nanoparticle-Polymer Composite Materials. *ACS Nano* **2014**, *8*, 9799−9806.
(23) Al-Nasassrah, M. A.; Podczeck, F.; Newton, J. M. The Effect of an Increase in Chain Length on the Mechanical Properties of Polyethylene Glycols. *Eur. J. Pharm. Biopharm.* **1998**, *46*, 31−38.

DOI: 10.1021/acsami.6b12086
ACS Appl. Mater. Interfaces 2016, 8, 33394−33398